

A DISCONTINUITY IN THE LOW-MASS INITIAL MASS FUNCTION

INGO THIES¹ & PAVEL KROUPA¹

Accepted 2007 August 10

ABSTRACT

The origin of brown dwarfs (BDs) is still an unsolved mystery. While the standard model describes the formation of BDs and stars in a similar way recent data on the multiplicity properties of stars and BDs show them to have different binary distribution functions. Here we show that proper treatment of these uncovers a discontinuity of the multiplicity-corrected mass distribution in the very-low-mass star (VLMS) and BD mass regime. A continuous IMF can be discarded with extremely high confidence. This suggests that VLMSs and BDs on the one hand, and stars on the other, are two correlated but disjoint populations with different dynamical histories. The analysis presented here suggests that about one BD forms per five stars and that the BD-star binary fraction is about 2%–3% among stellar systems.

Subject headings: binaries: general — open clusters and associations: general — stars: low-mass, brown dwarfs — stars: luminosity function, mass function

1. INTRODUCTION

Traditionally, brown dwarfs (BDs) are defined as (sub)stellar bodies with masses below the hydrogen burning mass limit (HBL), $m_{\text{H}} = 0.075 M_{\odot}$ for solar composition, and consequently they cool indefinitely after formation (Burrows et al. 1993; Chabrier & Baraffe 2000). Several attempts have been made to explain the formation of BDs by the same mechanisms as for stars, i.e. via fragmentation of a gas cloud and subsequent accretion (Adams & Fatuzzo 1996; Padoan & Nordlund 2002, 2004). If a gas cloud in a star-forming region fragments there will be a certain number of gas clumps with masses below the HBL. Unless the mass of the fragment is below the local Jeans mass it will contract in essentially the same way as higher mass clumps and finally produce a single or multiple BD. This scenario predicts similar multiplicities and also a substellar initial mass function (IMF) as a continuous extension of the stellar one (e.g. the standard model with BDs in Kroupa et al. 2003).

However, recent observations have shown that there is a lack of BD companions to low-mass stars (McCarthy, Zuckerman & Becklin 2003). Grether & Lineweaver (2006) found a star-BD binary fraction among solar-type primaries of less than 1% for close companions, the *brown dwarf desert*. This implies two populations of stellar and substellar objects, and that binaries are formed in each population separately (except for pairing due to post-formation dynamical exchanges). Observations e.g. by Reid et al. (2006) also show that most BD binaries have a primary-to-companion mass ratio of $q > 0.8$, in contrast to the mass ratio distribution of stellar binaries which has typically $q < 0.4$ (Duquennoy & Mayor 1991).

There are indications, e.g. Metchev & Hillenbrand (2005), that the BD desert may not be as dry for larger separations (> 30 AU) as it is for smaller ones. Since new surveys using adaptive optics or new instruments like the upcoming James Webb Space Telescope might reveal more substellar companions to stars, the fraction of star-BD systems may increase.

Apart from the BD desert there are more hints for a separate population. For example, BDs and VLMSs have a relatively low binary fraction of about 15%

(Bouy et al. 2003; Close et al. 2003; Martín et al. 2003; Kraus, White & Hillenbrand 2006; Law et al. 2007). By comparison, the stellar binary fraction is close to 100% for the very young Taurus-Auriga association (TA, about 1 Myr; Duchêne 1999; Luhman et al. 2003) and about 40%–50% for other clusters and field stars (Lada 2006). The BD and VLMS binary fraction can be increased to a starlike binary fraction if there are a large fraction of $\lesssim 5$ AU binaries, e.g. as deduced by Jeffries & Maxted (2005). But such a semi-major axis distribution would again imply a discontinuity of its form between low-mass stars and VLMSs/BDs and is not supported by the radial-velocity survey of Joergens (2006). We therefore do not consider the starlike formation as a major mechanism for BDs.

It has also been argued that the low binary fraction of BDs can be understood as a continuous extension of a trend that can already be recognized from G dwarfs to M dwarfs (Luhman 2004a; Sterzik & Durisen 2003). Therefore, the binary fraction alone cannot be taken as a strong evidence to introduce a separate population.

The most striking evidence for two separate populations is the empirical fact that the distribution of the separations and therefore the binding energies of BD binaries differs significantly from that in the stellar regime (Bouy et al. 2003; Burgasser et al. 2003; Martín et al. 2003; Close et al. 2003). This is shown in Figures 1 and 2. The solid line is a Gaussian fit to the central peak of the histogram while the dash-dotted one refers to (Basri & Reiners 2006, a compressed Fischer & Marcy 1992 fit). BDs and very low-mass stars (VLMS) have a semi-major axis distribution limited to $\lesssim 15$ AU, whereas M, K, and G dwarfs have a very broad and similar distribution (*long-dashed and short-dashed curves*; Close et al. 2003; Law, Hodgkin & Mackay 2007; Goodwin et al. 2007). There is also a dearth of BDs below 1 AU. Recent findings, e.g. by Guenther & Wuchterl (2003) and Kenyon et al. (2005), suggest a low number of such very close BD/VLMSs binaries. The semi-major axis distribution of BDs/VLMSs binaries based on the data from Close et al. (2003) can be modelled with a log a Gaussian centered at 4.6 AU ($\log a = 0.66$) with a half-peak width of $\sigma = 0.4$. It corresponds to an overall BD/VLMS binary fraction of $f_{\text{BD-BD}} = 0.15$. If data from Luhman (2004b), Joergens (2006), and Konopacky et al. (2007) are taken as

¹ Argelander-Institut für Astronomie (Sternwarte), Universität Bonn, Auf dem Hügel 71, D-53121 Bonn, Germany

hints to incomplete data between about 0.02 and 1 AU, the compressed Fischer & Marcy (1992) Gaussian from Figure 4 in Basri & Reiners (2006) may provide an appropriate envelope. However, for an assumed BD mass of $0.07 M_{\odot}$ and $f_{\text{BD-BD}} = 0.26$ their period distribution corresponds to a semi-major axis distribution with $\sigma \approx 0.85$ and is therefore still inconsistent with that of M and G dwarfs.

Although Konopacky et al. (2007) have recently found five VLMS binaries in TA with four of them having separations much larger than 15 AU, the sudden change of the orbital properties remains. In particular, they found two binaries with projected separations slightly above 30 AU and two others with separations between 80 and 90 AU. Possible implications of these discoveries are discussed in § 5.4. However, the truncation near 15 AU cannot be derived from the stellar distribution through downsizing according to Newton’s laws (Close et al. 2003; Bouy et al. 2003). Not even dynamical encounters in dense stellar environments can invoke such a truncation near 15 AU (Burgasser et al. 2003). Using N -body simulations Kroupa et al. (2003) tested the hypothesis that BDs and stars form alike, and mix in pairs, and found that, despite of close dynamical encounters, the distribution of the semimajor axes of BD binaries remains starlike. That is, dynamical encounters even in dense clusters cannot truncate the BD binary distribution near 15 AU. They further found that star-BD binaries would be much more frequent than actually observed. Thus, this classical hypothesis is rejected with high confidence.

With this contribution we study the implications of the observed change of binary properties on the underlying single-object initial mass function (IMF). For this purpose, we analyzed the observational mass functions of TA (Luhman et al. 2003a, 2004b), the IC 348 cluster (Luhman et al. 2003), the Trapezium cluster (Muench et al. 2002), and the Pleiades cluster based on data by Dobbie et al. (2002), Moraux et al. (2003), and the Prosser and Stauffer Open Cluster Database.² For all the systems we analyse, we refer to the MF as the IMF, although strictly speaking this is not correct for the 130 Myr old Pleiades. In § 2 we shortly review the definition of the IMF and the role of multiplicity on the shape of the individual body IMF compared to the observed system IMF (IMF_{sys}). We show that the IMF that can be derived from an observed IMF_{sys} does not need to be continuous even if the IMF_{sys} does not show any discontinuity. In § 3 we describe the statistical method how to fit a model IMF_{sys} by combining BD and star IMFs as an approximation to the observed IMF_{sys} . § 4 presents the results that indicate a discontinuity close to the HBL. Also the BD to star ratio from the model is calculated there. In § 5 the results are discussed in the context of four alternative BD formation scenarios, i.e. embryo ejection, disk fragmentation, photoevaporation, and ejection by close stellar encounters.

2. THE IMF FOR INDIVIDUAL STARS AND SYSTEMS

2.1. Definition

The IMF is among the most important properties of a stellar population since it gives hints to the processes that form stars and BDs. Although we can only observe stellar populations at their given age there are data of several very young populations where the mass function is probably still very close to the initial one.

² Available at <http://www.cfa.harvard.edu/~stauffer/opencl/>

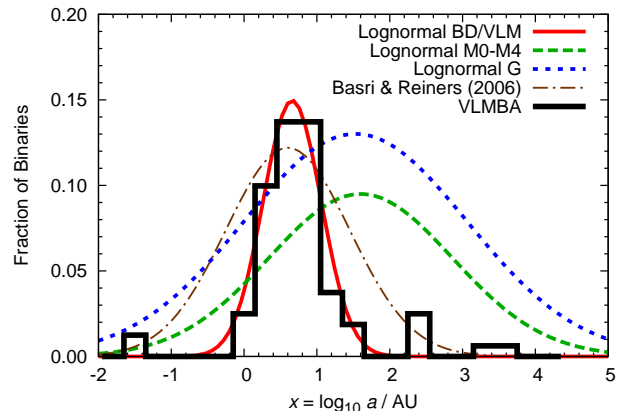


FIG. 1.— The semi-major axis (a) distribution for VLM binaries (VLMBs) with a total mass $m_{\text{bin}} < 0.2 M_{\odot}$ based on data from Nick Siegler’s *Very Low Mass Binaries Archive* (VLMBAs, http://paperclip.as.arizona.edu/~nsiegler/VLM_binaries/, version from June 1, 2007; histogram). The data can be fitted with a log-normal distribution. For the VLMBs (solid curve) the Gaussian parameters are $x_{\text{peak}} = 0.66$ (corresponding to $a = 4.6$ AU) and $\sigma = 0.4$ with a normalization factor (= total binary fraction) $f_{\text{tot}} = 0.15$, the binary fraction among BDs and VLMSs. For the M0–M4 dwarf binaries by Close et al. (2003) $x_{\text{peak}} = 1.6$ and $\sigma = 1.26$ ($f_{\text{tot}} = 0.3$) and for the G dwarf binaries $x_{\text{peak}} = 1.53$ and $\sigma = 1.53$ ($f_{\text{tot}} = 0.5$; Fischer & Marcy 1992, long-dashed and short-dashed curves, respectively). For VLMBs the gap within $-1.5 \leq \log a/\text{AU} \leq 0$ can be interpolated with the compressed Gaussian of Basri & Reiners (2006) with $\sigma = 0.85$ (thin dot-dashed curve), also enveloping wider BD/VLMS binaries found by Konopacky et al. (2007). It corresponds to a total BD/VLMS $f_{\text{BD-BD}} = 0.26$. The areas below the histogram and the curves are equal to the corresponding f_{tot} (eq. 3).

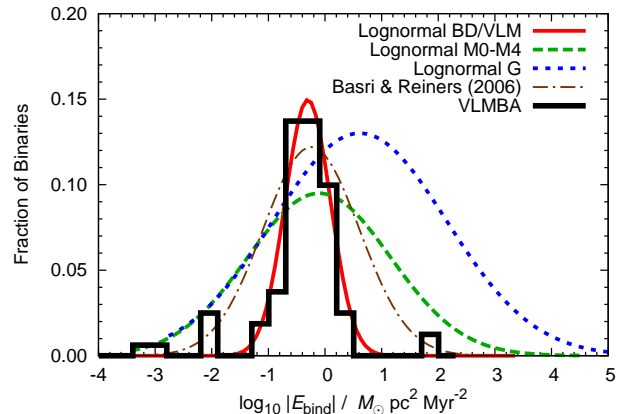


FIG. 2.— The distribution of the orbital binding energy $E_{\text{bind}} = -0.5G(m_1 m_2/a)$ for VLM binaries and low-mass stellar binaries. Line types and symbols are the same as in Fig. 1. As for the semi-major axes there is a clearly different distribution for BDs/VLMSs on the one hand side and M, K and G dwarf binaries on the other.

In general, the mass distribution of stars and BDs can be approximated by a power law or a combination of several power laws. Salpeter (1955) estimated the relationship between the stellar mass and the relative number of stars of a given mass as a single power law,

$$\xi(m) = \frac{dn}{dm} = k m^{-\alpha}, \quad (1)$$

for $0.4 \lesssim m/M_{\odot} \lesssim 10$ and with $\alpha = 2.35$ and a normalization constant k . The IMF is often expressed on the logarithmic mass scale and then becomes

$$\xi_{\text{L}}(\log m) = \frac{dn}{d \log m} = (\ln 10) m \xi(m) = k_{\text{L}} m^{1-\alpha}, \quad (2)$$

where k_L is the corresponding normalization constant for ξ_L . An IMF is said to be *flat* if $\xi_L(\log m)$ is constant, i.e. $\alpha = 1$. More recent work has shown there to be a flattening in the lower-mass regime of the observed mass function and, in the ξ_L representation, even a turnover near the BD-star transition (Kroupa 2001; Reid, Gizis & Hawley 2002; Chabrier 2003). Here, all objects from BDs to the most massive stars in a cluster are described by a *continuous IMF*, i.e. with a single population containing BDs as well as stars. The universal or “canonical” IMF has $\alpha_{BD} \equiv \alpha_0 = 0.3$ ($0.01 \leq m/M_\odot \leq 0.075$), $\alpha_1 = 1.3$ ($0.075 \leq m/M_\odot \leq 0.5$), and $\alpha_2 = 2.3$ ($0.5 \leq m/M_\odot \leq m_{\max}$), where m_{\max} is given by the mass of the host cluster (Weidner & Kroupa 2006). The generally accepted wisdom has been that the IMF is continuous from above $0.01 M_\odot$ to m_{\max} (e.g. Chabrier 2002).

2.2. Unresolved Binaries

Star cluster surveys are usually performed with wide-field telescopes with limited resolution that do not resolve most of the binaries. Hence, they yield, as an approximation, system MFs in which unresolved binary systems are counted as one object. The fraction of unresolved multiples can be taken as the total binary fraction of a cluster,

$$f_{\text{tot}} = \frac{N_{\text{bin,tot}}}{N_{\text{sng}} + N_{\text{bin,tot}}}, \quad (3)$$

where N_{sng} is the number of singles (or resolved individual bodies) and $N_{\text{bin,tot}}$ the number of (unresolved) binaries. Unresolved binaries increase the number of individual bodies, N_{bod} , in a cluster such that

$$N_{\text{bod}} = (1 + f_{\text{tot}})N_{\text{sys}}, \quad (4)$$

where $N_{\text{sys}} = N_{\text{sng}} + N_{\text{bin,tot}}$ is the total number of systems. Note that a “system” is either a single body or a binary or a higher order multiple. Here we ignore higher order multiples, because they are rare (Goodwin & Kroupa 2005). The binary fraction in dependence of the mass of the primary star, m_{prim} , is

$$f(m_{\text{prim}}) = \frac{N_{\text{bin,tot}}(m_{\text{prim}})}{N_{\text{sng}}(m_{\text{prim}}) + N_{\text{bin,tot}}(m_{\text{prim}})}, \quad (5)$$

where $N_{\text{bin,tot}}(m_{\text{prim}})$ and $N_{\text{sng}}(m_{\text{prim}})$ are, respectively, the number of binaries with primary star mass m_{prim} and single stars of mass m_{prim} .

2.3. The System Mass Function

The effect of this *binary error* on the appearance of the IMF can be described as follows. Assume a stellar population with $f_{\text{tot}} < 1$ and with stellar masses with a minimum mass m_{\min} and a maximum mass limit of m_{\max} . The minimum mass of a binary is $2m_{\min}$, while the mass-dependent binary fraction $f(m) = 0$ for $m_{\min} \leq m_{\text{sys}} < 2m_{\min}$. A binary closely above $2m_{\min}$ can only consist of two stars near m_{\min} making such binaries rare. For higher system masses, where a system can be a multiple or a single star, there are more possible combinations of primary and companion mass, so that the binary fraction increases with the system mass and approaches an upper limit for the most massive objects.

Figure 3 shows the general shape of a system IMF for a flat (logarithmic scale) IMF with $m_{\min} = 0.1 M_\odot$, $m_{\max} = 1 M_\odot$, and $f_{\text{tot}} = 0.5$. The IMF_{sys} is flat between m_{\min} and $2m_{\min}$ ($\log m/M_\odot \approx -0.7$) and rises above $2m_{\min}$ to a maximum at m_{\max} . Systems with $m_{\text{sys}} < 2m_{\min}$ can only be singles and the IMF_{sys} in this region is just the IMF minus the mass function

of objects that are bound to a multiple system. For masses $m_{\text{sys}} > m_{\max}$, on the other hand, only binaries exist, and the IMF_{sys} declines towards zero at $m_{\text{sys}} = 2m_{\max}$, the highest mass possible for binaries. The sharp truncation of the IMF at $m = m_{\max}$ causes the sudden drop at $m_{\text{sys}} = m_{\max}$, while the minor peak at $m_{\text{sys}} = m_{\max} + m_{\min}$ corresponds to the maximum of the *binary mass function* (IMF_{bin} , the IMF of binary system masses). For a binary of this mass the primary and companion mass can be drawn from the whole IMF, and thus the number of possible combinations becomes maximal. It should be noted that natural distributions with smoother boundaries probably do not show such a double peak.

Mathematically and in the case of random pairing, which is a reasonable approximation in the stellar regime (Malkov & Zinnecker 2001; Goodwin, Kroupa, Goodman & Burkert 2007), the binary mass function is just the integral of the product of the normalized IMF, $\hat{\xi} \equiv \xi/N_{\text{bod}}$, of each component times the total number of binaries $N_{\text{bin,tot}}$. Given the masses of the binary components A and B, m_A and m_B , the binary mass $m_{\text{bin}} = m_A + m_B$. Thus, $m_B = m_{\text{bin}} - m_A$. Thus, IMF_{bin} can now be written as

$$\xi_{\text{bin}}(m_{\text{bin}}) = N_{\text{bin,tot}} \int_{m_{\min}}^{m_{\text{bin}} - m_{\min}} \hat{\xi}(m) \hat{\xi}(m_{\text{bin}} - m) dm, \quad (6)$$

where m_{\min} is the lower mass limit of all individual bodies in the population. The upper limit of the integral, $m_{\text{bin}} - m_{\min}$, is the maximum mass of the primary component m_A corresponding to a secondary component with $m_B = m_{\min}$.

The other extreme case of assigning the component masses is equal-mass pairing. In that case, equation (6) simplifies to the IMF of one of the components and IMF_{bin} is just the IMF shifted by a factor of 2 in mass and corrected for binarity using equations (3) and (4):

$$\xi_{\text{bin,equal}}(m_{\text{bin}} = 2m) = \frac{f_{\text{tot}}}{1 + f_{\text{tot}}} \xi(m). \quad (7)$$

This case is more applicable for BD binaries since their mass ratio distribution peaks at a ratio $q = 1$ (Reid et al. 2006). However, due to the low overall binary fraction of BDs the effect of the mass ratio distribution is quite small.

The IMF_{sys} is just the sum of IMF_{bin} and the IMF of the remaining single objects, $(1 - f_{\text{tot}})\xi$:

$$\xi_{\text{sys}}(m) = \xi_{\text{bin}}(m) + (1 - f_{\text{tot}}) \xi(m). \quad (8)$$

Thus, to obtain the true individual star IMF, $\xi(m)$ has to be extracted from the observed $\xi_{\text{sys}}(m)$ for which a model for $\xi_{\text{bin}}(m)$ is required. That is IMF_{sys} has to be corrected for unresolved binaries in the cluster or population under study. This leads to a significant increase of the numbers of objects at the low-mass end because low-mass objects contribute to both low-mass singles and intermediate-mass binaries and thus more individual objects are required to reproduce the observed IMF_{sys} (Kroupa et al. 1991; Malkov & Zinnecker 2001). In the mass range $m_{\min} - 2m_{\min}$, systems can only be single because the system mass is the sum of the masses of the system members. Increasing the system mass beyond $2m_{\min}$ causes the binary contribution to rise quickly and then to asymptotically approximate a maximum value. Thus, the fraction of singles among M dwarfs is higher than for G dwarfs (Lada 2006), as one would expect for a stellar population ($> 0.08 M_\odot$), i.e. essentially without BDs.

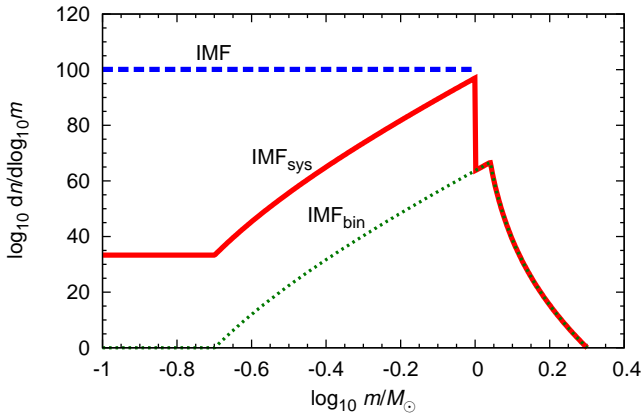


FIG. 3.— The system IMF (IMF_{sys} solid line) corresponding to a flat logarithmic IMF (i.e. $\alpha = 1$, dashed line) for $m_{\text{min}} = 0.1 \leq m/M_{\odot} \leq 1 = m_{\text{max}}$ with an overall binary fraction of 50%. The corresponding binary IMF (IMF_{bin} eq. 6) is shown by the thin dotted line. The system MF peaks at $1 M_{\odot}$ and is truncated for higher masses while there is a minor peak at $1.1 M_{\odot}$ corresponding to the peak of the binary MF at $m_{\text{min}} + m_{\text{max}}$.

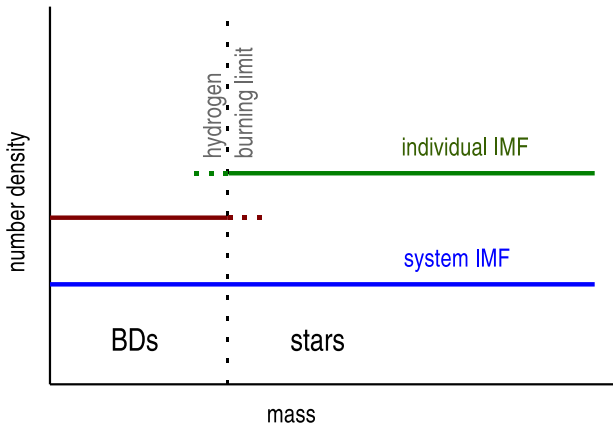


FIG. 4.— A population of stars and BDs with different binary fractions can result in a discontinuous IMF, even if the observed (system) IMF appears to be continuous. The binary fraction of the BDs is lower than that of stars and therefore a lower number, N_{bod} , of individual objects is required for the frequency of BD and stellar systems of a given mass being equal (eq. 4). Note the overlap region indicated by the horizontal dotted lines: some starlike bodies may actually be physical BDs (upper line) while some BD-likes are indeed very-low-mass stars.

Figure 4 schematically shows the effects of correcting a flat continuous observed IMF_{sys} for unresolved multiples whereby the binary fraction for BDs is smaller than for stars, as is observed to be the case. For a binary fraction of 15% (i.e. $f_{\text{BD-BD}} = 0.15$) among BDs there would thus be $N_{\text{BD}} = (1 + f_{\text{BD-BD}})N_{\text{sys,BD}} = 1.15N_{\text{sys,BD}}$ BDs in total, while for stars with $f_{\text{tot}} = 0.5$ we would have $1.5N_{\text{sys,star}}$. This exemplifies how the change in f leads to a discontinuous IMF_{sys} .

3. THE METHOD

3.1. The Parameter Space

The most straightforward way to calculate the influence of binaries on the stellar/substellar statistics would be the Monte Carlo method (Kroupa et al. 1991, 1993). However, for better (smoother) results and to reduce the computational efforts we do not use a Monte Carlo approach here but a semianalytical approach in which the binary mass function is calculated via numerical integration of eq. (6) for each population.

TABLE 1

LIST OF THE VARIABLE PARAMETERS THAT SPAN THE PARAMETER SPACE OF A TWO-POPULATION IMF STUDIED IN THIS CONTRIBUTION. NOTE THAT α_{BD} IS NOT VARIED FOR IC 348 AND THE PLEIADES SINCE IT IS NOT WELL-CONSTRAINED BY THE DATA FOR THESE CLUSTERS.

Parameter No.	Quantity	varied from	to (approx.)
1	α_{BD}	0	1
2	$m_{\text{max,BD}}$	$m_{0,\text{star}}$	$m_{0,\text{star}} + 0.2$
3	$\log \mathcal{R}_{\text{pop}}$	-1	0

TABLE 2

SIZE OF THE OBSERVED SAMPLE, N_{sys} (= THE NUMBER OF OBSERVED SYSTEMS), NUMBER OF DATA POINTS (MASS BINS), n_{data} , NUMBER OF FITTING PARAMETERS, c , AND THE NUMBER OF DEGREES OF FREEDOM, $\nu = n_{\text{data}} - 1 - c$, FOR THE FOUR CLUSTERS UNDER STUDY.

Cluster	N_{sys}	n_{data}	c	ν
Trapezium	1040	30	3	26
TA	127	9	3	5
IC 348	194	9	2	6
Pleiades	~ 500	19	2	16

This can be done with a standard quadrature algorithm. This algorithm has been verified with a Monte Carlo simulation of a few million random experiments, each being a random draw from the IMF. The Monte Carlo method is used later to determine the BD-to-star ratio and the total binary fractions within defined mass ranges (§§ 4.2 and 4.3). It makes use of the *Mersenne Twister* random number generator developed by Matsumoto & Nishimura (1998). Since there are only a few runs to be done (in contrast to hundreds of thousands of runs during an iterated parameter scan, see below) the simple Monte Carlo approach with an appropriately large random sample is fully sufficient for this purpose.

The lack of star-BD binaries and the truncation of the BD binary separation distribution suggest two disjunct populations where binary components are taken only from the same population. For reasons discussed in § 5 we call these populations *BD-like* and *starlike*. The binary corrections are therefore applied separately to the stellar and the substellar regime rather than to a combined population. Random pairing over the whole mass regime is not considered further as it leads to too many star-BD binaries (Kroupa et al. 2003).

The approach here requires separate application of normalizations on both populations. For this purpose we define the *population ratio*,

$$\mathcal{R}_{\text{pop}} = N_1/N_2 \quad (9)$$

where N_1 is the number of individual bodies of the BD-like population ($m_{0,\text{BD}} \leq m \leq m_{\text{max,BD}}$) and N_2 ($m_{0,\text{star}} \leq m \leq m_{\text{max}}$) that of the starlike population. This must not be mixed up with the *BD-to-star ratio*, \mathcal{R} , (eq. [14]) which refers to *physical* BDs and stars separated by the HBL.

The partial IMF for each population can be described by parameters α_i , m_j , and a normalization constant. In this work a single power law for BDs ($i = \text{“BD”}$) and a two-part power law ($i=1$ or 2) for stars is applied. Thus, there is a mass border, m_{12} , separating the two power law regimes. The parameters of both populations form a three-dimensional parameter space of the IMF model for each cluster. It has been found that the lower mass limits of the BD-like population, $m_{0,\text{BD}} = 0.01 M_{\odot}$,

and that of the starlike population, $m_{0,\text{star}} = 0.07 M_\odot$, are suitable for all studied clusters. Furthermore, we focus on the canonical stellar IMF (Kroupa 2001) with $\alpha_1 = 1.3$ for $m \leq 0.5 M_\odot \equiv m_{12}$ and $\alpha_2 = 2.3$ for $m > 0.5 M_\odot$. The reason is that this canonical IMF has been verified with high confidence by other observations as well as theoretically. Thus, only the BD-like power law, α_{BD} , the normalization of the BD-like population against the stellar one, \mathcal{R}_{pop} , and the upper mass border, $m_{\text{max,BD}}$, of the BD-like regime are the parameters to be varied. Because of the sparse and probably incomplete data sets for IC 348 and the Pleiades, α_{BD} has also been set to the canonical value (i.e. $\alpha_{\text{BD}} = \alpha_0 = 0.3$) for these clusters, varying only \mathcal{R}_{pop} and $m_{\text{max,BD}}$.

Table 1 lists the variables and their range of variation for the Trapezium, IC 348, and the Pleiades. As the upper mass limits of stars in the clusters one can either take the maximum observed mass or a theoretical mass limit, as given by Weidner & Kroupa (2006). Because in our model the IMF is cut sharply rather than declining softly as shown in that work, we here set the mass limit somewhat below the Weidner & Kroupa (2006) limits. For the Trapezium we set an upper limit of $10 M_\odot$, $1.5 M_\odot$ for TA, $3 M_\odot$ for IC 348 and $5 M_\odot$ for the Pleiades. Note that the observed most massive star in the Trapezium has a mass of $\approx 50 M_\odot$, but varying m_{max} to this value does not affect the results significantly.

Little is known about nonplanetary substellar objects below the standard opacity limit for fragmentation, $0.01 M_\odot$, making this a reasonable lower mass limit for our BD statistics. The lower-mass limit for stars, however, is chosen somewhat arbitrarily but is justified by a smaller test study that finds less agreement with observational data used here if the stellar mass is lowered too much below $0.08 M_\odot$. As will be shown later, the extreme case of a stellar mass range that includes the BD mass range leads to poor fits to the observational MFs as well as to some inconsistency with the observed binary fraction. This is discussed later in §§ 4 and 5. In general, the choice of the mass ranges also influences the mass ratio distribution, since for random-pairing each component is distributed via the IMF. Thus, for a given primary mass out of a chosen population, the companion mass distribution is just equal to $\xi(m)$ within the mass interval $m_{\text{min}} \leq m \leq m_{\text{prim}}$.

The overall binary fraction is taken as a constant for each population. For the stars we adopt an unresolved binary fraction of 80% for TA ($f_{\text{star-star}} = 0.80$) and 40% for the others ($f_{\text{star-star}} = 0.40$), in accordance to the observational data. For BDs we choose a value of 15% for all cases ($f_{\text{BD-BD}} = 0.15$). Furthermore, we found the need to introduce an overlap of the BD and star regimes between 0.07 and about $0.15\text{--}0.2 M_\odot$. Indeed, there is no reason why the upper mass border of the BD-like population should coincide with the lower mass border of the starlike population. The physical implications of this required overlap region are discussed in § 5.

3.2. χ^2 Minimization

In § 3.1 a parameter space of three (Trapezium, TA) and two (IC 348, Pleiades) dimensions of individually adjustable quantities has been defined. For each cluster, the quality of a set of fitting parameters is characterized via the χ^2 criterion,

$$\chi^2 = \sum_i^{n_{\text{data}}} \frac{(N_i - N \xi_{\text{sys}}(m_i))^2}{\sigma_i^2}, \quad (10)$$

where $\xi_{\text{sys}}(m_i)$ is IMF_{sys} at the midpoint of the i th bin of the observational histogram that is taken as the reference and n_{data}

is the number of mass bins in the observational histogram (Tab. 2). The values σ_i represent the error bars of the observational data, or, if none are given, the Poisson errors, and N_i is the number of systems found in the i th mass bin. The fitted IMF_{sys} is normalized to the total number of systems in the cluster.

That set of c fitting parameters that minimizes the reduced χ^2 value, $\chi_\nu^2 = \chi^2/\nu$, defines our best-fit model. Here $\nu = n_{\text{data}} - c - 1$ is the number of degrees of freedom. The values for n_{data} , c , ν , and the sample sizes for the studied clusters are listed in Table 2. The reduction of ν by 1 is due to the normalization of the total number of stars and BDs against the observational data. For the two-component model the fitting parameters are the power in the BD regime, α_{BD} , the upper mass border of the BD population, and the ratio \mathcal{R}_{pop} ; thus, $c = 3$ (2, for IC 348 and the Pleiades). The probability, P , that the model has a reduced χ^2 , $\chi_\nu^2 = \chi^2/\nu$, as large as or larger than the value actually obtained is calculated from the incomplete Gamma function (Press et al. 1992),

$$Q(\chi_\nu^2 | \nu) = P(\tilde{\chi}_\nu^2 \leq \chi_\nu^2). \quad (11)$$

The logarithmic mass error is not mentioned in the sources, but is given by the photometric measurements and to a larger degree by uncertain theoretical models of stars and BDs. We assumed a value of $\Delta \log m = 0.05$ for the Trapezium and $\Delta \log m = 0.1$ for the others, corresponding to a relative error in the mass estimates of 12% and 26%, respectively. This error has been estimated from the width of the logarithmic bins in the observational data for the Trapezium, TA and IC 348. For the Pleiades, for which non-equally spaced data from different sources are given, we assume the same log mass error as for TA, and IC 348. To take this into account the $\log m$ values have been smoothed by a Gaussian convolution corresponding to a lognormal smearing of the masses.

After generating the model IMFs for both populations a binary mass function (eq. [6]) is derived separately from the stellar and substellar IMF, i.e. there are formally no BD-like companions to starlike primaries, in accordance with the observations. This leads to consistency with the observed binary fraction (§ 4.3) and the BD desert. Note, though, that as a result of the required overlap both the BD-like and the starlike population contain stars as well as BDs; thus, we do have star-BD pairs in our description (more on this in § 5).

The addition of the two resulting system IMFs leads to an overall IMF_{sys} for the whole mass range. By adjusting the power law coefficients and the population ratio \mathcal{R}_{pop} , the IMF_{sys} is fitted against the observational data such that χ^2 is minimized. The prominent substellar peak in the Trapezium cluster below $0.03 M_\odot$ (Muench et al. 2002) is ignored here because it is well below the BD–star mass limit and therefore does not interfere with any feature there. Furthermore, it is possibly an artefact of the BD mass–luminosity relation (Lada & Lada 2003).

3.3. Error Estimation

The errors of the parameters are estimated from the marginal distribution of each parameter within the parameter space (Lupton 1993). The marginal probability density distribution, p , is

$$\begin{aligned} p(A_i) &= \text{d}P(A_i)/\text{d}A_i \\ &= \int_{-\infty}^{\infty} \int_{-\infty}^{\infty} \mathcal{L}(A_1, A_2, A_3) \text{d}A_k \text{d}A_j, \end{aligned} \quad (12)$$

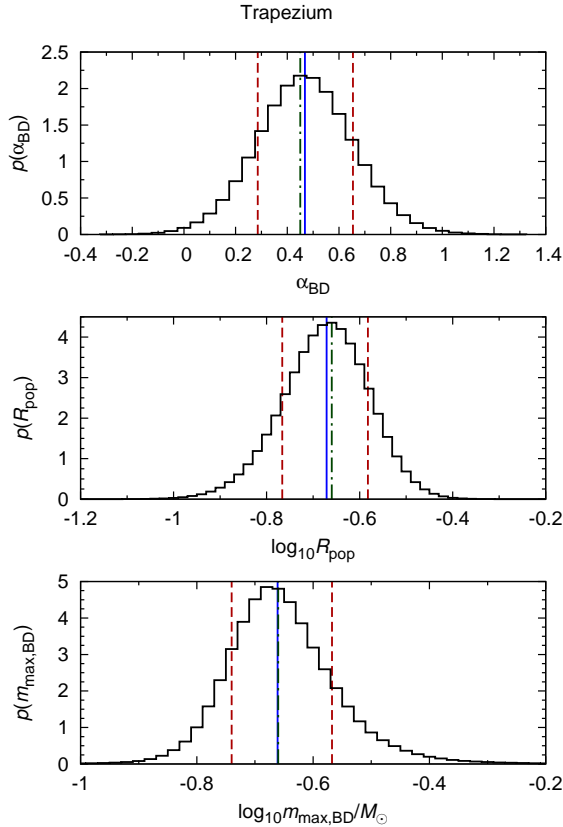


FIG. 5.— The marginal probability density distributions of the parameters α_{BD} , $\log_{10} \mathcal{R}_{\text{pop}}$ and $\log(m_{\text{max,BD}}/M_{\odot})$ as an estimate of the errors for the Trapezium cluster fit (see § 3.3). The peak-width engulfing 68% of the whole parameter sample (thus referring to $\approx 1\sigma$, dashed vertical lines) is taken as the error for each parameter. Because the median (solid vertical line) of the sample does not match the best-fit value (dash-dotted line) in all cases, both are listed in Table 3.

where A_1, A_2 and A_3 correspond to α_{BD} , \mathcal{R}_{pop} , $m_{\text{max,BD}}$ and $i = 1, \dots, 3; j, k \neq i$. The likelihood \mathcal{L} is defined as

$$\mathcal{L}(A_1, A_2, A_3) = \mathcal{N} e^{-\chi^2/2}, \quad (13)$$

where the normalization constant \mathcal{N} is such that the integral over the whole range is one. Note that χ^2 instead of χ_{ν}^2 is used here. The integral is approximated by summation with equidistant stepping of each parameter. We conservatively rejected all parameter sets with $P < 0.27\%$ (corresponding to $\chi_{\nu}^2 > \pm 3\sigma$; § 3.2).

As an example, the parameter distribution for the Trapezium is illustrated in Figure 5. The interval around the median which contains 68% of the scanned parameter sets is taken as the σ measure of the errors. The interval limits and the medians are shown among the best-fit results in Table 3. Apparently, the median of the probability density distribution does not always coincide with the best-fit value. The reason for this is that the distribution is slightly asymmetric for most parameters and clusters with the Pleiades being the by far worst case. This results in asymmetric error bars. Note that there are sets of α_{BD} , \mathcal{R}_{pop} , and $m_{\text{max,BD}}$ that are within these error limits but with a $\chi^2 > 3\sigma$, and thus the error limits may be slightly over-estimated.

Another possibility to illustrate the statistical significance of a fit is by its confidence contours within a two-dimensional subspace of the parameter space, as is shown later in § 4.2.

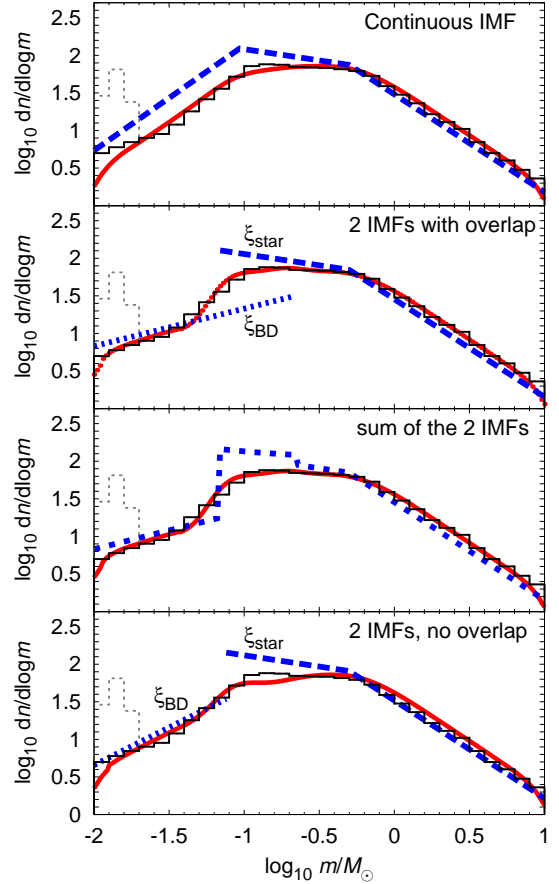


FIG. 6.— Four different IMF models applied to the Trapezium cluster. Top panel: A classical continuous-IMF fit (dashed line) for the Trapezium cluster with random pairing over the whole BD and stellar mass range. The method of converting the IMF to the IMF_{sys} (solid curve) is essentially the same as for the two-component IMFs discussed in this paper but with no allowance for an overlap or a discontinuity in the BD-star transition region. Although the general shape of the observational histogram (thin steps) is represented by this fit this model leads to an unrealistic high fraction of star-BD binaries and is therefore discarded. Second panel: The Trapezium IMF fitted with two separate IMFs, ξ_{BD} (dotted line) and ξ_{star} (dashed line), as in Figure 7 (the two-component IMF). Third panel: The same but with the sum IMF of both component IMFs shown here as the possible appearance of the IMF if all binaries could be resolved. Apparently, there is a “hump” between about $0.07 M_{\odot}$ and $0.2 M_{\odot}$ bracketing the probable overlap region of the BD-like and starlike populations. Bottom panel: Trapezium fitted with two separate IMFs but with no overlap. The binary correction leads to the dip near the hydrogen-burning limit. However, the fit is only slightly worse than that one with an overlap.

4. RESULTS

4.1. The IMF for BDs and Stars

Figure 6 demonstrates the results for different models (continuous IMF, two-component IMF with and without overlap region) for the Trapezium cluster. The continuous IMF is shown for illustration only. Its underlying model assumes a single population containing BDs as well as stars (Kroupa et al. 2003). Instead of an overlap as for the two-component model the mass border between the regime of the BD slope α_{BD} and the (canonical) stellar regime is varied. The total binary fraction, f_{tot} , is set to 0.4 with random pairing among the entire population. Our calculations give a best fit with $\alpha_{\text{BD}} = -0.4 \pm 0.2$, $m_{\text{max,BD}} \equiv m_{0,\text{star}} = 0.093 \pm 0.01$ (and canonical stellar IMF) which is comparable to the canonical IMF for BDs and stars (Kroupa 2001). As already mentioned in § 1, it leads to a high number of star-BD binaries,

TABLE 3
THE BEST-FIT BD-LIKE POWER LAW COEFFICIENTS, α_{BD} , POPULATION RATIOS, \mathcal{R}_{pop} , AND BD-LIKE UPPER MASS LIMITS, $m_{\text{max,BD}}$. THE UNCERTAINTIES ARE DERIVED IN § 3. NOTE THAT α_{BD} IS SET TO THE CANONICAL VALUE FOR IC 348 AND THE PLEIADES.

Cluster	Median $\pm 1\sigma$			Best fit			χ^2_ν	P
	α_{BD}	$\log \mathcal{R}_{\text{pop}}$	$m_{\text{max,BD}}$	α_{BD}	$\log \mathcal{R}_{\text{pop}}$	$m_{\text{max,BD}}$		
Trapezium	$0.47^{+0.18}_{-0.19}$	$-0.67^{+0.10}_{-0.09}$	$0.22^{+0.04}_{-0.05}$	0.45	-0.66	0.22	0.23	0.99998
TA	$-0.08^{+0.63}_{-1.05}$	$-0.68^{+0.13}_{-0.14}$	$0.11^{+0.03}_{-0.04}$	0.00	-0.62	0.12	2.69	0.020
IC 348	—	$-0.57^{+0.23}_{-0.19}$	$0.22^{+0.06}_{-0.08}$	0.3 (c)	-0.51	0.22	1.01	0.416
Pleiades	—	$-0.82^{+0.44}_{-0.11}$	$0.07^{+0.02}_{-0.20}$	0.3 (c)	-0.80	0.06	1.20	0.257

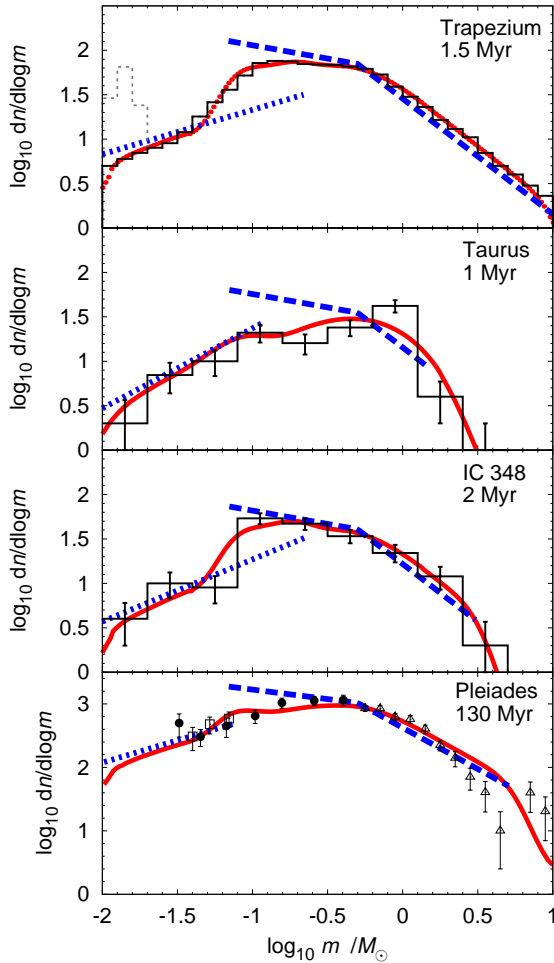


FIG. 7.— Two-component IMFs of the Trapezium, IC 348, and TA clusters based on observational data by Luhman (2004a), Luhman et al. (2003) and Muench et al. (2002) (solid histograms), as well as for the Pleiades cluster using data from Moraux et al. (2003) (filled circles), Dobbie et al. (2002) (open squares) and from the Prosser and Stauffer Open Cluster Database (from which only those for $\log m/M_\odot \leq 0.55$ are used for fitting). For all clusters the stellar IMF, shown here as the dashed line, has the canonical or standard shape after Kroupa (2001), i.e. $\alpha_1 = 1.3$ below $0.5 M_\odot$ and $\alpha_2 = 2.3$ above $0.5 M_\odot$. The Trapezium IMF is fitted without the substellar peak indicated by the faint dotted steps. The dotted lines show the optimized binary-corrected BD-like body IMFs (distribution of individual BD-like bodies). The resulting model system IMFs are represented by the solid curves. Ages are from Luhman et al. (2003), Luhman et al. (2003), Hillenbrand et al. (2001) and Barrado y Navascués et al. (2004) for TA, IC 348, Trapezium and the Pleiades, respectively. Note that the BD-like IMF of IC 348 and the Pleiades are set to the canonical slope $\alpha_{\text{BD}} = 0.3$ since they are not well constrained due to the lack of BD data for these clusters.

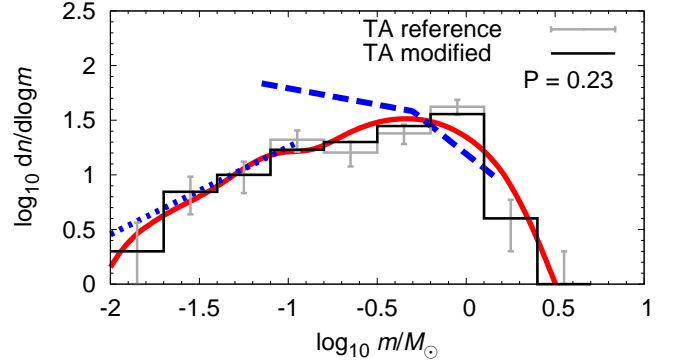


FIG. 8.— The two-component model with canonical stellar IMF for a slightly modified TA observational histogram (black solid steps). The peak at $1 M_\odot$ and the dent around $0.3 M_\odot$ have been slightly flattened without leaving the error bars of the original data (grey steps and bars). This fit has a reasonable confidence of about $P = 0.25$, about 12 times larger than for the original histogram ($P = 0.02$, see Tab. 3).

$f_{\text{star-BD}} = 15\% \pm 4\%$ altogether (see §4.3), while Kroupa et al. (2003) found 7%–15% star-BD binaries with $a \gtrsim 30$ AU in their standard model with stars and BDs. Furthermore, the different orbital properties of BD-BD and star-star binaries (Fig. 1) cannot be explained by a single-population model without further assumptions. Therefore, it is not considered further here.

The two-component IMF model (Fig. 6, *second panel*) accounts for the empirical binary properties of BDs and stars. Apart from this it also fits the observational data (Fig. 6, *histogram*) slightly better than the continuous model, especially in the BD/VLMS region and the “plateau” between 0.1 and $0.5 M_\odot$.

Objects with equal mass and composition appear as equal in observations, even if they have been formed in different populations. Thus, it is hard to determine their formation history. A high-resolution survey that resolves most of the multiples would yield an overall mass function from the lowest mass BDs to the highest mass stars. However, if such a resolved individual mass function is composed of two overlapping populations, it may be possible to detect its imprints as an excess of objects within the overlap region. To illustrate this ((Fig. 6, *third panel*), we construct such an overall IMF by simply adding the two IMF components from the second panel. BDs and stars are paired separately from their respective mass range. It is clear that the addition of the two IMFs leads to discontinuities, i.e. in the overlap region the continuous IMF increases steeply at the minimum stellar mass and drops again at the upper mass limit of the BD-like regime. Even with a smoother drop at each end of the BD-like and starlike IMF it is likely to be detectable once most of the multiples have been resolved. Thus, a discovery of such a

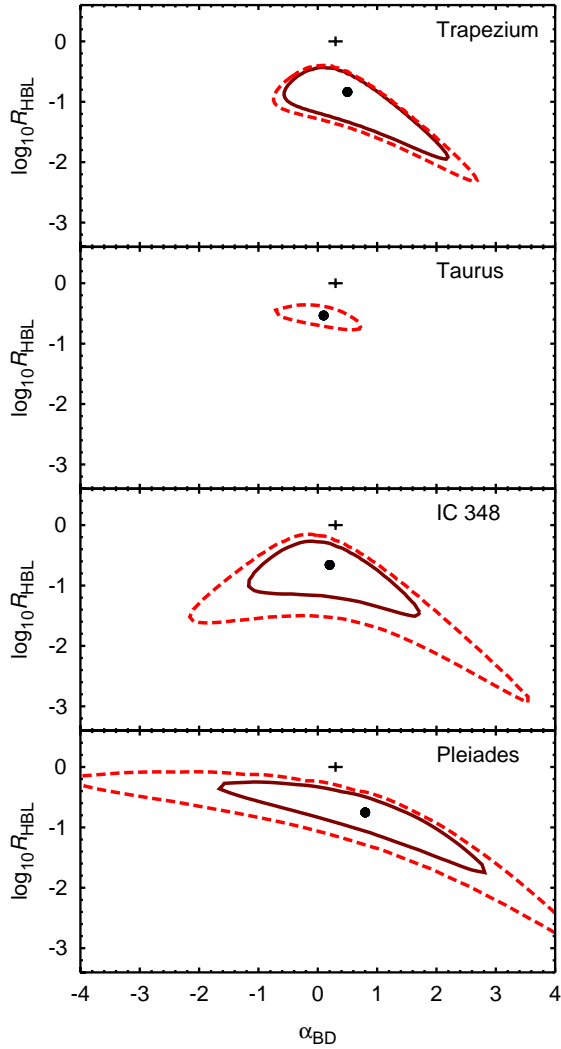


FIG. 9.— Contour plots of 5% and 1% significance levels from χ^2 fitting (see § 3 for details) of α_{BD} and the BD-like to starlike ratio \mathcal{R}_{HBL} at $m = 0.075 M_{\odot}$ (eq. 15) for the Trapezium, TA, IC 348 and the Pleiades. The stellar IMF is canonical, i.e. $\alpha_1 = 1.3$ and $\alpha_2 = 2.3$ while the upper BD mass limits, $m_{\text{max,BD}}$, are the best-fit values from Table 3. All fitting parameters outside the solid line are rejected with 95%, and those outside the dashed line are rejected with 99% confidence. The optimum of the Trapezium and TA is marked by the filled circle while the cross marks the standard/canonical configuration with a continuous IMF (i.e. $\log \mathcal{R}_{\text{HBL}} = 0$) and $\alpha_{\text{BD}} = 0.3$. As can be seen, it is well outside both levels (even for arbitrary α_{BD}). For the Pleiades it is still well outside at least for reasonable choices of α_{BD} . Note that the optimum for α_{BD} for IC 348 and the Pleiades does exist in this 2D cross section but not in the full 3D parameter space.

“hump” within the resolved IMF would strongly support the two-component model.

To illustrate the effect of the overlap region, a two-component IMF without an overlap is shown in the bottom panel of Figure 6. Like the continuous IMF this approach gives a slightly worse fit, especially between 0.1 and $0.2 M_{\odot}$ ($-1 \leq \log m/M_{\odot} \leq -0.7$). However, the “dip” in this region is only weak.

The results of the two-component IMF model for all clusters are shown in Figure 7, the power law coefficients being listed in Table 3. For the Pleiades and IC 348 the BD IMF slope has been kept standard, i.e. $\alpha_{\text{BD}} = 0.3$ (Kroupa 2001), because the sparse, and in the case of the Pleiades most probably incomplete data, do not allow useful confidence limits to be placed on α_{BD} . For the same reason the highly uncertain

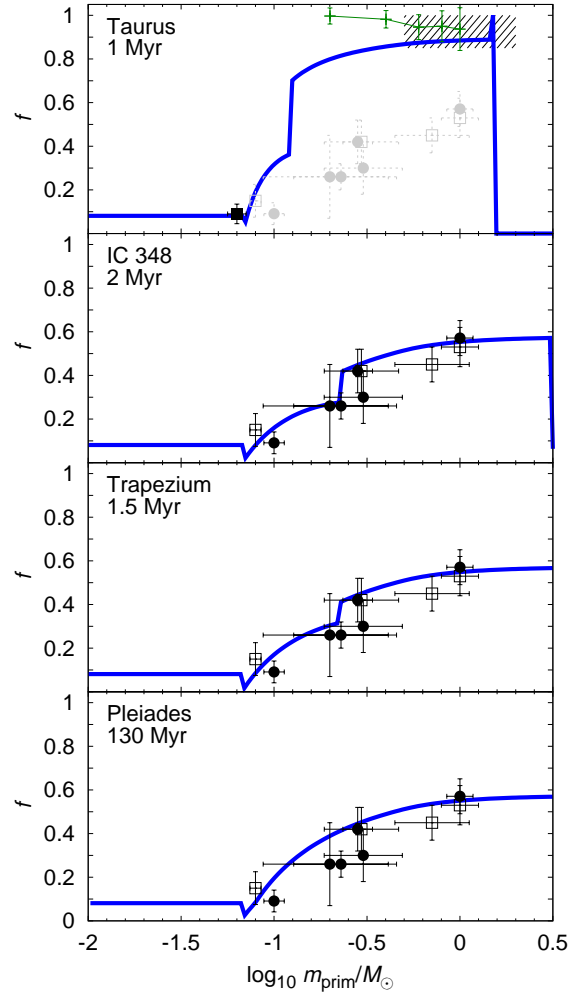


FIG. 10.— The binary fraction f (eq. 5) of the four discussed clusters as a function of primary mass, m_{prim} , for the two-component best-fit IMF model (with canonical stellar IMF) is shown by the solid line. The BD binary fraction appears flat due to the equal-mass pairing used in our algorithm. Since merely very sparse data is available for low-mass BDs, only the higher-mass end of the curve should be taken into account. For comparison, the average binary fractions of G, K, M and L type stars in the solar neighbourhood (average age ~ 5 Gyr; filled circles: Lada 2006, open squares: Kroupa et al. 2003) have been added to each panel. The shaded region in the top panel indicates the approx. 1 Myr old pre-main sequence data (Duchêne 1999) while the thin solid line represents the initial TA-like dynamical model from Kroupa et al. (2003). The single filled square in the top panel at $\log m \approx -1.2$ is the VLMS/BD datum inferred by Kraus et al. (2006) for TA. Note that the stars in TA have a binary fraction near 100% (Duchêne 1999; Kroupa et al. 2003).

observational data for $\log(m/M_{\odot}) \geq 0.65$ have not been used for fitting (but are still plotted for completeness).

As can be seen the BD/VLMS and stellar IMFs do not meet at the BD-star boundary. The number density of individual BDs near the BD-star border is about one third of that of individual low-mass M dwarfs. This discontinuity cannot be seen directly in the observational data because it is masked by the different binary fractions for different masses (§2.3), but the IC 348 data (histogram in the third panel of Figure 7) may indeed be showing the discontinuity (compare third panel of Figure 6).

Furthermore, there are large uncertainties in the mass determination of stars in stellar groups such as TA which may probably lead to even larger error bars of the bins than shown in the observational data. Even within the given error bars

certain variations of these data provide a much better fit to the canonical stellar IMF with $P = 0.25$ (original: $P = 0.02$, Table 3). This has been done in Figure 8 by lowering the peak near $1 M_{\odot}$ and somewhat rising the “valley” around $0.3 M_{\odot}$ corresponding to the re-shuffling of 9 stars out of 127 (Tab. 1) by 0.1 to $0.4 M_{\odot}$ (one bin width), e.g. through measurement errors. This suggests that, in agreement with Kroupa et al. (2003), the TA IMF might not necessarily be inconsistent with the canonical IMF.

Except for the Pleiades all clusters show features near the peak in the low-mass star region that are slightly better fitted with a separate BD population *and* an overlap region. Although these features alone do not reject the continuous IMF model, they might be taken as a further support of the argumentation towards a two-populations model.

It should be mentioned that the continuous IMF model (Fig. 6, *first panel*) still fits the observed Trapezium and Pleiades MF with high confidence (while failing for the other clusters) but leads to VLMS binary properties that are inconsistent with the observed properties as mentioned in § 1. A possible extension of our modelling would thus be to fit both the observed IMF *and* the observed binary statistics.

4.2. BD to Star Ratio

We analyzed the BD-to-star ratio \mathcal{R} of TA, Trapezium and IC 348, defined as

$$\mathcal{R} = \frac{N(0.02-0.075M_{\odot})}{N(0.15-1.0M_{\odot})}, \quad (14)$$

where N is the number of bodies in the respective mass range. The mass ranges are chosen to match those used in Kroupa & Bouvier (2003) in their definition of \mathcal{R} . Since BDs below $0.02 M_{\odot}$ are very difficult to observe and since TA and IC 348 do not host many stars above $1 M_{\odot}$ (in contrast to Trapezium and the Pleiades), we restricted the mass ranges to these limits.

The Pleiades cluster is difficult to handle due to a lack of BD data. Moreover, at an age of about 130 Myr (Barrado y Navascués, Stauffer & Jayawardhana 2004) it has undergone dynamical evolution, and massive stars have already evolved from the main sequence which affects the higher mass end of the IMF (Moraux et al. 2004).

Another relevant quantity is the ratio \mathcal{R}_{HBL} of BD-like to starlike objects at the HBL, i.e. the classical BD-star border,

$$\mathcal{R}_{\text{HBL}} = \frac{\xi_{\text{BD}}(0.075M_{\odot})}{\xi_{\text{star}}(0.075M_{\odot})}. \quad (15)$$

In the classical continuous IMF approach it is one by definition, because otherwise the IMF would not be continuous. In a two-component IMF its value depends on the shapes of the BD-like and the starlike IMF, as well as on the BD-to-star ratio. The evaluation of equation (15) yields $\mathcal{R}_{\text{HBL}} = 0.17$ for the Trapezium, $\mathcal{R}_{\text{HBL}} = 0.30$ for TA, $\mathcal{R}_{\text{HBL}} = 0.22$ for IC 348, and $\mathcal{R}_{\text{HBL}} = 0.3$ for the Pleiades. Although \mathcal{R}_{HBL} is not an input parameter here but is calculated from the two IMFs and their relative normalization, \mathcal{R}_{pop} , it could easily be used as one instead of \mathcal{R}_{pop} while calculating the latter from \mathcal{R}_{HBL} .

Figure 9 shows the contour plots of the 5% and 1% significance ranges in the $\alpha_{\text{BD}} - \mathcal{R}_{\text{HBL}}$ space for Trapezium, TA, IC 348, and the Pleiades. The significance values are calculated from χ^2_{ν} via the incomplete Gamma function as described in § 3. The contours mark the regions outside which the hypothesis of a two-component IMF with a single power

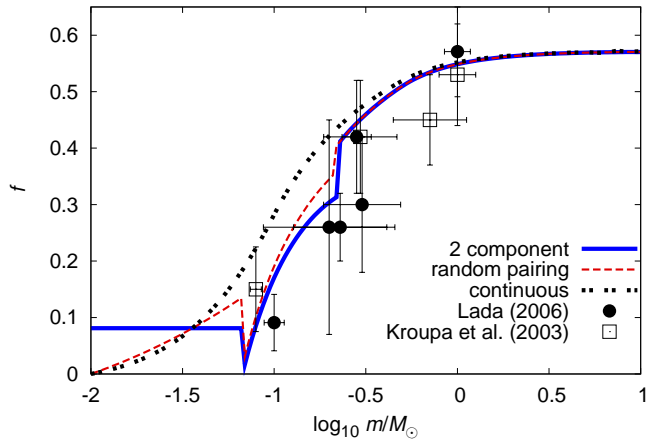


FIG. 11.— The binary fraction $f(m_{\text{prim}})$ of our best 2-component IMF fit for the Trapezium (solid line) with $\alpha_{\text{BD}} = 0.5$ in comparison with the binary fraction, $f_c(m_{\text{prim}})$, of the best continuous IMF model (dotted line, see also top panel in Figure 6). The 2-component model assumes random pairing of stars but equal-mass pairing for BD binaries. The continuous model, on the other hand, assumes random pairing of companions chosen randomly from the canonical IMF ($\alpha_{\text{BD}} = 0.3$, $\alpha_1 = 1.3$ and $\alpha_2 = 2.3$). This model is merely shown for illustrative purposes and has already been discarded (§ 1). The thin dashed line refers to the same two-component IMF as the solid line, but with random-pairing instead of equal-mass pairing for BDs. The visible jumps in $f(m_{\text{prim}})$ at $\log(m/M_{\odot}) = -1.15$ and -0.7 are due to the truncation at the upper and lower mass limit of the BD-like and the starlike population with their different binary properties. The global shapes of the continuous and the two-component IMF curves are similar but $f_c(m_{\text{prim}})$ is significantly higher than $f(m_{\text{prim}})$ in the low-mass star and VLMS regime and outside the uncertainties of the data by Lada (2006).

law for BDs and a double power law for stars has to be rejected with 95% or 99% confidence. Also shown (by a cross) is the standard configuration with $\alpha_{\text{BD}} = 0.3$ and $\log \mathcal{R}_{\text{HBL}} = 0$ for the continuous standard IMF. This point is outside both levels for all three clusters, and at least for Trapezium and TA it is well outside even for arbitrary α_{BD} . In other words, *the corresponding hypothesis of a continuous IMF has to be rejected with at least 99% confidence.*

The size of the non-rejection areas can be used for an estimate of the errors of α_{BD} and \mathcal{R}_{HBL} . However, one has to keep in mind that these are only maximum possible deviations with all the other parameters kept at the optimum. The non-rejection areas in the full three-dimensional parameter space are therefore expected to be somewhat narrower.

4.3. Binary Fraction

Additionally, the binary fraction for each cluster as well as the total binary fraction is calculated for the best-fit models. The fraction of binaries as a function of the primary mass, $f(m_{\text{prim}})$, among all systems is shown in Figure 10. For stars the binary fraction is a monotonic function of the primary mass in agreement with the data (Lada 2006), at least for the Trapezium, IC 348, and the Pleiades. For BDs, however, it is flat due to the equal-mass pairing. In the case of random pairing it would approach zero for very low mass BDs (Fig. 11). The true mass ratio function grows monotonically with the mass ratio and becomes very steep near $q = 1$, as shown by Reid et al. (2006). Thus, for BDs the true binary fraction is probably closer to the equal-mass case than the random pairing case.

For comparison, Figure 11 also shows the binary fraction, $f_c(m_{\text{prim}})$, for the Trapezium that would result from a continuous IMF. Although the overall shape is very similar to that of the two-component model the binary fraction near the BD-

star transition is significantly higher for low-mass stars than the observed values while being approximately equal for stars above $1 M_{\odot}$. Thus, a continuous IMF cannot fit the observational data as good as a two-population IMF even if f_{tot} is reduced.

The total fractions of BD-BD binaries, $f_{\text{BD-BD}}$, of star-star binaries, $f_{\text{star-star}}$, and the fraction of (very low mass) star-BD binaries, $f_{\text{star-BD}}$, are of further interest. Pairs of the latter type consist of two objects of the *BD-like* or *starlike* population (see § 5 for the motivation and definition of the populations) but where the primary object is a star ($m_{\text{prim}} \geq 0.075 M_{\odot}$) within the BD-VLMS overlap region between 0.07 and $0.15 M_{\odot}$, while the companion is a true, physical BD with a mass below $0.075 M_{\odot}$.

For each cluster we define

$$f_{\text{BD-BD}} = \frac{N_{\text{BD-BD}}}{N_{\text{sys,BD}}} \quad (16)$$

$$f_{\text{MD-MD}} = \frac{N_{\text{MD-MD}}}{N_{\text{sys,MD}}} \quad (17)$$

$$f_{\text{star-star}} = \frac{N_{\text{star-star}}}{N_{\text{sys,star}}} \quad (18)$$

$$f_{\text{star-BD}} = \frac{N_{\text{star-BD}}}{N_{\text{sys,star}}}, \quad (19)$$

where $N_{\text{BD-BD}}$ is the number of all BD-BD binaries (i.e. all objects have masses $\leq 0.075 M_{\odot}$), $N_{\text{MD-MD}}$ that of all M dwarf-M dwarf (MD-MD) binaries, $N_{\text{star-star}}$ that of all star-star binaries, and $N_{\text{star-BD}}$ the number of mixed (star-BD) binaries (composed of a VLMS and a BD). Furthermore, $N_{\text{sys,BD}}$ is the number of all BD systems (including single BDs), $N_{\text{sys,MD}}$ that of all M dwarf systems, and $N_{\text{sys,star}}$ the number of all systems with a star as primary and with a stellar, BD, or no companion. As for the BD-to-star ratio we also applied the (primary) mass ranges from Kroupa & Bouvier (2003) on the BD and star sample from each cluster but with no gap between the BD and the stellar regime, i.e. $0.02 M_{\odot} \leq m_{\text{prim}} \leq 0.075 M_{\odot}$ for BDs and $0.075 M_{\odot} \leq m_{\text{prim}} \leq 1 M_{\odot}$ for stars. In addition, the binary fraction of M dwarfs is calculated in the same way as the stellar one but in the mass range $0.075 M_{\odot} \leq m_{\text{prim}} \leq 0.5 M_{\odot}$. The uncertainty limits of the binary fractions and BD-to-star ratios have been derived from those of the IMF slopes by applying the minimum and maximum slopes.

The results are shown in Table 4. The binary fractions for BDs vary only slightly between 12% and 15%, while the stellar binary fraction, $f_{\text{star-star}}$, is about 70% for TA and 30%–40% for the others. They are apparently slightly lower than the binary fractions that are set for the starlike population because of the nonconstant distribution binary as shown in Figure 10. The binary mass function (eq. [6]) is smaller in the mass region below $1 M_{\odot}$ and thus the binarity is below average if the focus is set on this region.

Furthermore, in the overlap region the relatively low binary fraction of VLMSs from the BD-like population also contributes to $f_{\text{star-star}}$, which results in an even lower value of $f_{\text{star-star}}$. This trend is more emphasized for the M dwarf binary fraction, $f_{\text{MD-MD}}$, which is about 10% lower than $f_{\text{star-star}}$ for each cluster but still much larger than $f_{\text{BD-BD}}$.

The star-BD binary fraction $f_{\text{star-BD}}$ is of special interest since it is the measure for the “dryness” of the BD desert. Note that due to the equal-mass pairing used here for BD-like binaries, the BD-like population formally does not contribute to $f_{\text{star-BD}}$. All star-BD binaries are from the starlike regime

which extends down to $m_{0,\text{star}} = 0.07 M_{\odot}$, i.e. into the BD mass regime. For the Trapezium, IC 348, and the Pleiades our two-component models yield values between 2% and 2.5%, whereas TA shows $f_{\text{star-BD}} \approx 5\%$. For comparison, the continuous IMF from the top panel of Figure 6 corresponds to $f_{\text{star-BD}} = 15\% \pm 4\%$. For mass ratio distributions other than equal-mass pairing we expect a higher $f_{\text{star-BD}}$, consisting mostly of binaries from the BD-like population with primary masses slightly above the HBL and companion masses below. For random pairing of BD-like binaries this increment is between 0.01 and 0.03. Also the lower mass limit of the starlike population slightly influences f_{tot} . It should also be noted that the size of the error limits for $f_{\text{star-BD}}$ are calculated from the uncertainties of the IMF model (Tab. 3) but do not include the uncertainties of $m_{0,\text{star}}$.

5. DISCUSSION: BROWN DWARFS AS A SEPARATE POPULATION?

5.1. An Apparent Discontinuity

By correcting the observed MFs for unresolved multiple systems a discontinuity in the IMF near the BD/VLMS region emerges. We have also tried to model continuous single-body IMFs, but we find this hypothesis of continuity to be inconsistent with the observed MFs given the observational data on the binary properties of stars and BDs. We have shown that the *empirically determined* difference in the binary properties between BDs/VLMSs on the one hand side and stars on the other, and the *empirical finding* that stars and BDs rarely pair, implies a discontinuity in the IMF near the BD/VLMSs mass.

Thus, the discontinuity in binary properties, which has already been interpreted to mean two separate populations (Kroupa & Bouvier 2003), also implies a discontinuity in the IMF. This relates the probably different formation mechanism more clearly to the observational evidence.

We have performed a parameter survey allowing the IMF parameters α_{BD} , \mathcal{R}_{pop} , and $m_{\text{max,BD}}$ to vary finding that the canonical stellar IMF ($\alpha_1 = 1.3$ and $\alpha_2 = 2.3$) cannot be discarded even for TA, and that the BD/VLMS discontinuity is required for all solutions. The discontinuity uncovered in this way, if measured at the classical BD-star border, is of a similar magnitude for the stellar clusters studied ($0.17 \leq \mathcal{R}_{\text{HBL}} \leq 0.30$), supporting the concept of a universal IMF, which is, by itself, rather notable.

We recommend calling these populations *BD-like* and *starlike* with respect to their formation history. These populations have probably overlapping mass ranges since there is no physical reason for the upper mass limit of the BD-like population to match the lower mass limit of the starlike one. Furthermore, the best-fit models suggest such an overlap between $0.07 M_{\odot}$ and about $0.2 M_{\odot}$. According to this classification through the formation history, BD-like objects would include VLMSs, while starlike ones would include massive BDs.

The overlap region implies that BD-like pairs can consist of a VLMS-BD pair, and that a starlike binary can consist of a stellar primary with a massive BD as a companion. As can be seen from Table 4, the star-BD fractions are similar (except for the dynamically unevolved TA) and that the star-BD binary fraction, $f_{\text{star-BD}}$, is about 2%–3%. This is somewhat higher than the value of $< 1\%$ BD companion fraction Grether & Lineweaver (2006) found for nearby stars but still far below the value expected for a single population model (at least 7%–15% in Kroupa et al. 2003 and $15\% \pm 4\%$ in our calculations). Simulations by Bate et al. (2003), Bate & Bonnell

TABLE 4

BINARY FRACTIONS $f_{\text{BD-BD}}$ FOR BD-BD, $f_{\text{MD-MD}}$ FOR MD-MD, $f_{\text{star-BD}}$ FOR STAR-BD AND $f_{\text{star-star}}$ FOR STAR-STAR BINARIES IN THE STUDIED CLUSTERS. NOTE THAT THE STAR-BD BINARIES RESULT FROM THE PAIRING IN THE OVERLAP REGION BETWEEN ABOUT 0.075 AND $0.15 M_{\odot}$. THUS, FOR EXAMPLE, IN IC 348 2.1% OF ALL STARS ARE EXPECTED TO HAVE A PHYSICAL BD AS A COMPANION. IN ADDITION, THE BD-TO-STAR RATIO BETWEEN 0.02 AND $1.0 M_{\odot}$ \mathcal{R} , AND AT THE HBL, \mathcal{R}_{HBL} , IS LISTED. NOTE THAT THE NUMERICAL UNCERTAINTIES OF $f_{\text{star-BD}}$ ARE PROBABLY MUCH SMALLER THAN TRUE ONES SINCE $f_{\text{star-BD}}$ LARGELY DEPENDS ON $m_{0,\text{star}}$.

Cluster	$f_{\text{BD-BD}}$	$f_{\text{MD-MD}}$	$f_{\text{star-star}}$	$f_{\text{star-BD}}$	\mathcal{R}	\mathcal{R}_{HBL}
Trapezium	0.13 ± 0.01	0.30 ± 0.01	0.34 ± 0.01	0.023 ± 0.002	0.18 ± 0.03	0.17 ± 0.04
TA	0.15 ± 0.01	0.64 ± 0.06	0.69 ± 0.05	0.046 ± 0.005	0.27 ± 0.09	0.30 ± 0.11
IC 348	0.13 ± 0.02	0.29 ± 0.02	0.33 ± 0.02	0.021 ± 0.004	0.20 ± 0.10	0.22 ± 0.11
Pleiades	0.13 ± 0.02	0.33 ± 0.03	0.37 ± 0.03	0.025 ± 0.002	0.28 ± 0.18	0.28 ± 0.18

(2005), and Bate (2005) predict a fraction of about 2% star-BD binaries (actually one M dwarf with a BD companion out of 58 stars formed in three independent calculations). Note that, in our model, $f_{\text{star-BD}}$ is a prediction of the required overlap region and is sensitive to the overlapping range. As our model for the Pleiades IMF suggests, the overlapping range might be considerably smaller than that we have found for the other clusters. Furthermore, we did not fit the lower mass border, $m_{0,\text{star}}$, of the starlike population but simply assumed a value of $0.07 M_{\odot}$ which is well in the BD mass regime (and is the major source of star-BD binaries in our Pleiades model). A slight increase of $m_{0,\text{star}}$ by only $0.01 M_{\odot}$ would cause the Pleiades star-BD binary fraction to drop to nearly zero.

Several authors doubt the existence of two separate populations. Most recently, Eislöffel & Steinacker (2007) summarize that the observational community in general prefers the model of starlike formation for BDs. They mention the detection of isolated proto(sub)stellar “blobs” in the Ophiuchus B and D clouds, which may support the theory of starlike formation for BDs. It remains unclear, though, how many of these blobs will actually form BDs instead of dissolving from lack of gravitational binding energy. Goodwin & Whitworth (2007) refer to a private communication with Å. Nordlund stating that the pure turbulence theory predicts about 20,000 transient cores for every actual pre-stellar core of about $0.1 M_{\odot}$.

We recall that one of the main reasons for the existence of a separate population is the semi-major axis distribution of BD binaries (Fig. 1). But Luhman et al. (2007) also mention a wide binary BD in Ophiuchus with a separation of approximately 300 AU. Indeed, a small number of wide BD binaries are known. However, it can be doubted that the occasional discovery of a wide BD binary may expand the narrow semi-major axis distribution (Fig. 1) to a starlike one. The striking evidence posed by the lack of BD companions to stars is a strong indication for two populations. It is usually ignored by the community, though. We note that even if there actually may be some BDs that formed starlike they are most probably a minority.

There is also the interpretation of the BD desert being a “low- q desert” rather than an absolute mass-dependent drop in the companion mass function. Grether & Lineweaver (2006) find a low-mass companion desert of solar-type primary stars between approximately 0.01 and $0.06 M_{\odot}$. They find this interval to be dependent on the primary star mass and therefore predict M dwarfs to have BD companions, and that M dwarfs ought to have a companion desert between a few Jupiter masses and the low-mass BD regime. However, this interpretation does not address the different orbital properties of

BDs and stars as well as the different q distribution.

5.2. Implications for the Formation History

Can the existence of such a discontinuity, i.e. the formation of two separate populations, be understood theoretically? Although BDs and stars appear to be distinct populations the formation of BDs is likely to be connected to star formation. Bate et al. (2002, 2003) show that BDs significantly below $0.07 M_{\odot}$ cannot form in a classical way since the minimum mass they need for stellar-type formation would also lead to progressive accretion and growth to stellar mass unless they are in regions with very low mass infall rates. But such regions are very rare, because the prevailing densities and temperatures cannot achieve the required Jeans masses, as also stressed by Goodwin & Whitworth (2007). For this reason, Adams & Fatuzzo (1996) expected BDs to be rare. Only a small fraction of the BDs, especially those at the high-mass end of the BD regime, may form this way if the surrounding gas has been consumed by star formation processes just after the proto-BD has reached the Jeans mass. To explain the actually higher BD frequency (per star) in recent surveys the accretion process has to be terminated or impeded somehow (Bonnell, Larson & Zinnecker 2007).

Also the above-mentioned differences in the distribution of the semimajor axes between BDs and stars cannot be explained by a scaled-down star formation process, because that would imply a continuous variation and a much broader semimajor axis distribution for BDs and VLMSs that has not been observed (Kroupa et al. 2003). While binary stars show a very broad distribution of their semimajor axes peaking at about 30 AU the semimajor axes of BDs are distributed around about 5 AU with a sharp truncation at 10–15 AU (Fig. 1). No smooth transition region between both regimes can be recognized (Close et al. 2003). In a high angular resolution survey Law et al. (2007) found that the orbital radius distribution of binaries with $V-K < 6.5$ appears to differ significantly from that of cooler (and thus lower mass) objects, suggesting a sudden change of the number of binaries wider than 10 AU at about the M5 spectral type. This is in agreement with our finding of a possible BD-like population that extends beyond the hydrogen-burning mass limit into the VLMS regime.

In a radial-velocity survey of Chamaleon I, Joergens (2006) has found evidence for a rather low binary fraction below 0.1 AU, while most companions found in that survey orbit their primaries within a few AU. For this reason an extreme excess of close BD binaries that cannot be resolved by imaging surveys appears to be unlikely. A larger binary fraction than about 15% would thus not be plausible. Basri & Reiners (2006) suggest an upper limit of $26\% \pm 10\%$ for the BD binary

fraction based on their own results ($11\%^{+0.07}_{-0.04}$, for separations below 6 AU) and the survey by Close et al. (2003; $15\% \pm 7\%$, for separations greater than 2.6 AU) by simple addition of the results. This is nearly consistent with a BD binary fraction of 15%, since the survey is neither magnitude- nor volume-limited. However, they admit that their value may be overestimated since the objects with separations between 2.6 and 6 AU are counted twice. We note further that even a total BD binary fraction of 25% ($f_{\text{BD-BD}} = 0.25$), although outside the error limits of our best-fit models, would only lead to a minor change in the fitted IMFs.

It has been argued (Basri & Reiners 2006) that the lower binary fraction of BDs is just the extension of a natural trend from G dwarfs to M dwarfs (Figs. 10 and 11). Our contribution has shown that this trend can be understood by the simple fact that there are many fewer possibilities to form a binary near the lower mass end than for higher component masses. The observational data are in better agreement with a minimum mass, m_{min} , near the hydrogen-burning mass limit and a low overall binary fraction of BD-like objects than with an “all-in-one” IMF from the lowest mass BDs to the upper stellar mass limit, as shown in Figure 11. This observed trend thus appears as an additional enforcement of the two-populations model of BDs and stars.

Given that the conditions for a starlike formation of BDs are very rare (Bate et al. 2003), four alternative formation scenarios for BDs apart from starlike formation can be identified, namely

1. Formation of wide star-BD binaries via fragmentation of a proto- or circumstellar disk and subsequent disruption by moderately close encounters.
2. Formation of BDs as unfinished stellar embryos ejected from their birth system.
3. Removal of the accretion envelopes from low-mass protostars via photoevaporation.
4. Removal of the accretion envelopes due to extremely close stellar encounters (Price & Podsiadlowski 1995).

Scenario 4 can be ruled out as the major BD formation mechanism because the probability of such close encounters, with required flyby distances typically below 10 AU (Kroupa & Bouvier 2003) for efficient disruption of accretion envelopes (less than a tenth of those proposed by Thies et al. [2005] for triggered planet formation), is far too low for such a scenario being a significant contribution to BD formation. The photo evaporation model, as studied by Whitworth & Zinnecker (2004), also cannot be the major mechanism of BD formation (Kroupa & Bouvier 2003). It predicts a variation of the IMF with the population number and density of the host cluster. In dense starburst clusters (young globular clusters) with a larger number of O/B stars or even modest clusters such as the ONC with a dozen O/B stars compared to TA, a larger fraction of low-mass stars would have halted in growth. This would result in a bias towards M dwarfs, since many of them would be failed K or G dwarfs. In contrast to this prediction, Briceño et al. (2002) and Kroupa et al. (2003) show that the IMFs of TA and ONC are very similar in the mass range $0.1\text{--}1 M_{\odot}$, while globular clusters likewise have a low-mass MF similar to the standard form (Kroupa 2001).

5.3. Embryo Ejection

Reipurth (2000) and Reipurth & Clarke (2001) introduced the formation of BDs as ejected stellar embryos as the alternative scenario 2. If a forming protostar in a newborn multiple system is ejected due to dynamical instability its accretion process is terminated and the object remains in a protostellar state with only a fraction of the mass compared to a fully developed star. Since the final mass is physically independent of the hydrogen fusion mass limit one would not expect the mass range of ejected embryos to be truncated at the HBL and thus expect an *overlap region* between these populations. This fully agrees with the requirement of having to introduce such an overlap region in order to fit the observed IMF_{sys} in § 3.

This model gives some hints to understand the low BD binary fraction as well as the truncation of the semimajor axis distribution of BDs. The decay of a young multiple system of three or more stellar embryos typically leads to the ejection of single objects but also to the ejection of a small fraction of close binaries. In order to survive the ejection, the semi-major axis of such a binary must be significantly smaller (by a factor of about 3) than the typical orbital separation within the original multiple system. A similar explanation is that the orbital velocity of the BD binary components has to be higher than the typical ejection velocity in order to keep the interaction cross section of the binary with other system members small. Indeed, the velocity dispersion of BDs in the embryo-ejection model shown in Kroupa & Bouvier (2003) is $\lesssim 2 \text{ km s}^{-1}$ for the majority of the BDs. This is in good agreement with the Keplerian orbital velocity of each BD-binary member of about $1.5\text{--}2 \text{ km s}^{-1}$ for an equal-mass binary of $0.05\text{--}0.08 M_{\odot}$ and $a \approx 10 \text{ AU}$. The majority of BD binaries have smaller separations, and, consequently, higher orbital velocities and are bound tighter. This would set the low binding energy cut near $E_{\text{bind}} = 0.2 \text{ pc}^{-2} \text{ Myr}^2$ in Figure 2.

There have been numerical simulations of star formation and dynamics, e.g. by Bate et al. (2003) and Umbreit et al. (2005), in which binaries are produced via ejection that show remarkably similar properties to the actually observed ones. Umbreit et al. (2005) describe the formation of BDs from decaying triple systems. Their simulations predict a semi-major axis distribution between about 0.2 and 8 AU (see Fig. 8 in their paper), peaking at 3 AU. This is slightly shifted towards closer separations compared with the results by Close et al. (2003) but still in agreement with the observational data. In contrast to this, Goodwin & Whitworth (2007) doubt the frequent formation of close BD binaries via ejection, arguing that hydrogen-burning stars which formed via ejection were almost always single.

In further qualitative support of the embryo ejection model, Guieu et al. (2006) describe a deficit by a factor of 2 of BDs near the highest density regions of TA relative to the BD abundance in the less dense regions that can possibly be explained by dynamical ejection and consequently larger velocity dispersion of stellar embryos, i.e. BDs. A starlike fragmentation scenario would result in an opposite trend since the Jeans mass is smaller for higher densities, thus allowing gas clumps of lower mass to form (sub)stellar bodies. Contrary to this, Luhman (2006) did not find any evidence for a different spatial distribution of BDs and stars in TA. Recently, Kumar & Schmeja (2007) have found that substellar objects in both the Trapezium and IC 348 are distributed homogeneously within twice the cluster core radii

while the stellar populations display a clustered distribution. They conclude that these distributions are best explained with a higher initial velocity dispersion of BDs, in accordance with Kroupa & Bouvier (2003), supporting the embryo-ejection model.

However, the embryo-ejection model has a challenge to reproduce the high fraction of significant disks around BDs that have been observed in young clusters. Several studies, e.g. Natta et al. (2004), reveal a considerable number of BDs with an infrared excess that indicates the presence of warm circum(sub)stellar material. While these studies do not show the actual mass of these disks because a small amount of dust in these disks is sufficient to produce these excesses, Scholz, Jayawardhana & Wood (2006) found 25% of BDs in TA having disks with radii > 10 AU and significant masses (larger than $0.4 M_J$). For the remaining 75% no disks were detectable. In simulations, e.g. by Bate et al. (2003), such large disks survive occasionally, but less frequently (about 5%) than suggested by the observations (Scholz et al. 2006). However, Scholz et al. (2006) point out that their results do not rule out the embryo-ejection scenario and admit that this mechanism may still be relevant for some BDs. In general, the embryo-ejection model is in agreement with at least the existence of low-mass circumsubstellar disks up to about 10 AU (Bate et al. 2003; Umbreit et al. 2005; Güdel et al. 2007). Thies et al. (2005) also show that a thin low-mass disk can survive near-parabolic prograde coplanar encounters above about three Hill radii with respect to the disk-hosting BD. This means that a disk with a radius up to about 5 AU (later viscously evolved to about 10 AU, see Bate et al. 2003) can survive a flyby of an equal-mass embryo within about 15 AU while larger disks or widely separated binaries would be disrupted.

Furthermore, Bate et al. (2003) suggest from their simulations that the binary fraction via ejection might be as small as about 5% (see also Whitworth et al. 2007).

5.4. Disk Fragmentation and Binary Disruption

The fragmentation of protobinary disks with subsequent disruption of a star-BD binary is another promising alternative scenario. A disk can fragment during the accretion process if it reaches a critical mass above which the disk becomes gravitationally unstable against small perturbations. Fragmentation may be triggered by an external perturbation, i.e. infalling gas clumps or a passing neighbor star. The latter mechanism may also be capable of triggering fragmentation in relatively low-mass circumstellar disks resulting in rapid planet formation (Thies et al. 2005). Thus, BD formation via disk fragmentation likely plays an important role in the early ages of the cluster where the frequency of massive disks is highest (Haisch et al. 2001; Whitworth et al. 2007).

Following the argumentation of Goodwin & Whitworth (2007), disk fragmentation may explain the observed distribution of BD binary separations at least as well as the embryo-ejection model. In addition, it may explain the existence of wide star-BD binaries, since a fraction of the initial wide binaries can survive without being disrupted. Because the likelihood of disrupting close encounters depends on the mass and density of the host cluster, one expects a higher fraction of those wide star-BD binaries in smaller and less dense clusters and associations like TA. However, further studies and observations are needed to test this hypothesis.

Whitworth & Stamatellos (2006) show that BDs can actually form as widely separated companions to low-mass stars

with mass m at a sufficiently large disk radius, r_{disk} ,

$$r_{\text{disk}} \gtrsim 150 \text{ AU} \left(\frac{m}{M_{\odot}} \right), \quad (20)$$

where the disk is cool enough to allow a substellar clump to undergo gravitational collapse. For a primary star below $0.2 M_{\odot}$ this minimum radius therefore becomes less than 90 AU which is in remarkable agreement with the two wider VLMS binaries found by Konopacky et al. (2007). Such large distances to the primary star allow the formation of BD-BD binaries as well as the survival of circumsubstellar disks up to about 10–30 AU, depending on the total mass of the pre-substellar core and the mass of the primary star. Furthermore, this scenario explains the existence of wide star-BD binaries. In addition, such a wide star-BD binary can be disrupted by moderately close encounters of about 100–200 AU (i.e. a distance similar to the star-BD orbital radius), the disruption of such systems appears to be likely in contrast to the disruption of accretion envelopes as required in the already rejected scenario 4.

5.5. Summary

Both the embryo-ejection model and disk fragmentation with subsequent wide binary disruption explain the above-mentioned connection between stars and BDs, since BDs start to form like stars before their growth is terminated due to their separation from their host system or from lack of surrounding material in the outer parts of a circumstellar disk. It is obvious that the formation rate of these embryos is proportional to the total star formation rate.

For these reasons these formation mechanisms appear to be the most likely ones for BDs and some VLMSs and BD/VLMS binaries. It cannot be decided yet which scenario is the dominant mechanism. This may depend on the size and the density of the star-forming region. We expect, on the other hand, the classical starlike formation scenario to be of some importance only for the most massive BDs.

The possibility of two different *alternative* BD formation mechanisms (disk fragmentation and embryo ejection) may lead to another discontinuity in the intermediate mass BD IMF since both scenarios correspond to different binary fractions as mentioned above. The currently available data, however, are far from being sufficient for a verification of this prediction.

6. CONCLUSIONS

The different empirical binary properties of BDs and stars strongly imply the existence of two separate but mutually related populations. We have shown that if the IMF of BDs and stars is analyzed under consideration of their binary properties then there is a discontinuity in the transition region between the substellar and stellar regime that is quite independent of the host cluster. The discontinuity in the IMF near the HBL is a strong logical implication of the disjunct binary properties and suggests splitting up the IMF into two components, the BD-like and the starlike regime. An alternative but equivalent description would be to view the stellar IMF as a continuous distribution function ranging from about 0.07 to $150 M_{\odot}$ (Weidner & Kroupa 2004), and a causally connected but disjoint distribution of (probably mostly) separated ultra-low-mass companions and ejected embryos with masses ranging from $0.01 M_{\odot}$ to 0.1 – $0.2 M_{\odot}$. While the canonical stellar IMF is consistent with the observed stellar MFs at least for

the Trapezium, IC 348, and the Pleiades, the sub-stellar IMF of at least the Trapezium and TA has a power law index that is consistent with the canonical value $\alpha_{BD} = 0.3$. Within the error limits, our analysis does not reject the canonical power law indices for BDs and stars for any cluster.

The discontinuity is often masked in the observational data due to a mass overlap of both populations in the BD-VLMS region as well as the higher apparent masses of unresolved binaries compared to single objects in the observed IMF_{sys}. The discontinuity in the number density near the HBL is a step of approximately a factor of 3–5 (Table 4). This implies a general dependency between both populations and is, as far as we can tell, consistent with the scenario of disrupted wide binaries (Goodwin & Whitworth 2007) as well as with the truncated-star scenario (e.g. as an ejected stellar embryo,

Reipurth & Clarke 2001), since the number of unready stars is directly correlated with the total amount of star formation in the host cluster. Both embryo-ejection and wide binary disruption are also consistent with the properties of close binary BDs.

Our results (Tab. 3) suggest that about one BD is produced per 4–6 formed stars. This suggests the necessity of a distinct description of BDs and stars as well as the connection between these two populations through their formation process.

ACKNOWLEDGEMENTS

This work was partially supported by the AIfA and partially by DFG grant KR1635/12-1.

REFERENCES

- Adams F. C., Fatuzzo M., 1996, *ApJ*, 464, 256
 Barrado y Navascués D., Stauffer J. R., Jayawardhana R., 2004, *ApJ*, 614, 386
 Basri G., Reiners A., 2006, *AJ*, 132, 663
 Bate M. R., 2005, *MNRAS*, 363, 363
 Bate M. R., Bonnell I. A., 2005, *MNRAS*, 356, 1201
 Bate M. R., Bonnell I. A., Bromm V., 2002, *MNRAS*, 332, L65
 Bate M. R., Bonnell I. A., Bromm V., 2003, *MNRAS*, 339, 577
 Bonnell I. A., Larson R. B., Zinnecker H., 2007, in Reipurth B., Jewitt D., Keil K., eds, *Protostars and Planets V The Origin of the Initial Mass Function*. pp 149–164
 Bouy H., Brandner W., Martín E. L., Delfosse X., Allard F., Basri G., 2003, *AJ*, 126, 1526
 Briceño C., Luhman K. L., Hartmann L., Stauffer J. R., Kirkpatrick J. D., 2002, *ApJ*, 580, 317
 Burgasser A. J., Kirkpatrick J. D., Reid I. N., Brown M. E., Miskey C. L., Gizis J. E., 2003, *ApJ*, 586, 512
 Burrows A., Hubbard W. B., Saumon D., Lunine J. I., 1993, *ApJ*, 406, 158
 Chabrier G., 2002, *ApJ*, 567, 304
 Chabrier G., 2003, *PASP*, 115, 763
 Chabrier G., Baraffe I., 2000, *ARA&A*, 38, 337
 Close L. M., Siegler N., Freed M., Biller B., 2003, *ApJ*, 587, 407
 Dobbie P. D., Pinfield D. J., Jameson R. F., Hodgkin S. T., 2002, *MNRAS*, 335, L79
 Duchêne G., 1999, *A&A*, 341, 547
 Duquennoy A., Mayor M., 1991, *A&A*, 248, 485
 Eislöffel J., Steinacker J., 2007, *ArXiv Astrophysics e-prints*
 Fischer D. A., Marcy G. W., 1992, *ApJ*, 396, 178
 Goodwin S. P., Kroupa P., 2005, *A&A*, 439, 565
 Goodwin S. P., Kroupa P., Goodman A., Burkert A., 2007, in Reipurth B., Jewitt D., Keil K., eds, *Protostars and Planets V The Fragmentation of Cores and the Initial Binary Population*. pp 133–147
 Goodwin S. P., Whitworth A., 2007, *A&A*, 466, 943
 Grether D., Lineweaver C. H., 2006, *ApJ*, 640, 1051
 Güdel M., Padgett D. L., Dougados C., 2007, in Reipurth B., Jewitt D., Keil K., eds, *Protostars and Planets V The Taurus Molecular Cloud: Multiwavelength Surveys with XMM-Newton, the Spitzer Space Telescope, and the Canada-France-Hawaii Telescope*. pp 329–344
 Guenther E. W., Wuchterl G., 2003, *A&A*, 401, 677
 Guieu S., Dougados C., Monin J.-L., Magnier E., Martín E. L., 2006, *A&A*, 446, 485
 Haisch K. E., Lada E. A., Lada C. J., 2001, *ApJ*, 553, L153
 Hillenbrand L. A., Carpenter J. M., Feigelson E. D., 2001, in Montmerle T., André P., eds, *ASP Conf. Ser. 243: From Darkness to Light: Origin and Evolution of Young Stellar Clusters The Orion Star-Forming Region*. pp 439–+
- Jeffries R. D., Maxted P. F. L., 2005, *Astronomische Nachrichten*, 326, 944
 Joergens V., 2006, *A&A*, 446, 1165
 Kenyon M. J., Jeffries R. D., Naylor T., Oliveira J. M., Maxted P. F. L., 2005, *MNRAS*, 356, 89
 Konopacky Q. M., Ghez A. M., Rice E. L., Duchene G., 2007, *ArXiv Astrophysics e-prints*
 Kraus A. L., White R. J., Hillenbrand L. A., 2006, *ApJ*, 649, 306
 Kroupa P., 2001, *MNRAS*, 322, 231
 Kroupa P., Bouvier J., 2003, *MNRAS*, 346, 369
 Kroupa P., Bouvier J., Duchêne G., Moraux E., 2003, *MNRAS*, 346, 354
 Kroupa P., Gilmore G., Tout C. A., 1991, *MNRAS*, 251, 293
 Kroupa P., Tout C. A., Gilmore G., 1993, *MNRAS*, 262, 545
 Kumar M. S. N., Schmeja S., 2007, *A&A*, 471, L33
 Lada C. J., 2006, *ApJ*, 640, L63
 Lada C. J., Lada E. A., 2003, *ARA&A*, 41, 57
 Law N. M., Hodgkin S. T., Mackay C. D., 2007, *ArXiv e-prints*, 704 (submitted to *MNRAS*)
 Luhman K. L., 2004a, *ApJ*, 617, 1216
 Luhman K. L., 2004b, *ApJ*, 614, 398
 Luhman K. L., 2006, *ApJ*, 645, 676
 Luhman K. L., Allers K. N., Jaffe D. T., Cushing M. C., Williams K. A., Slesnick C. L., Vacca W. D., 2007, *ApJ*, 659, 1629
 Luhman K. L., Briceño C., Stauffer J. R., Hartmann L., Barrado y Navascués D., Caldwell N., 2003, *ApJ*, 590, 348
 Luhman K. L., Stauffer J. R., Muench A. A., Rieke G. H., Lada E. A., Bouvier J., Lada C. J., 2003, *ApJ*, 593, 1093
 Lupton R., 1993, *Statistics in Theory and Practice*, first edn. Princeton University Press, Princeton, New Jersey
 Malkov O., Zinnecker H., 2001, *MNRAS*, 321, 149
 Martín E. L., Barrado y Navascués D., Baraffe I., Bouy H., Dahm S., 2003, *ApJ*, 594, 525
 Matsumoto M., Nishimura T., 1998, *ACM Trans. Model. Comput. Simul.*, 8, 3
 McCarthy C., Zuckerman B., Becklin E. E., 2003, in Martín E., ed., *IAU Symposium There is a Brown Dwarf Desert of Companions Orbiting Stars between 75 and 1000 AU*. pp 279–+
- Metchev S., Hillenbrand L., 2005, *Memorie della Societa Astronomica Italiana*, 76, 404
 Moraux E., Bouvier J., Stauffer J. R., Cuillandre J.-C., 2003, *A&A*, 400, 891
 Moraux E., Kroupa P., Bouvier J., 2004, *A&A*, 426, 75
 Muench A. A., Lada E. A., Lada C. J., Alves J., 2002, *ApJ*, 573, 366
 Natta A., Testi L., Muzerolle J., Randich S., Comerón F., Persi P., 2004, *A&A*, 424, 603
 Padoan P., Nordlund Å., 2002, *ApJ*, 576, 870
 Padoan P., Nordlund Å., 2004, *ApJ*, 617, 559
 Press W. H., Teukolsky S. A., Vetterling W. T., Flannery B. P., 1992, *Numerical Recipes in Fortran 77*, second edn. Cambridge University Press, Cambridge
 Price N. M., Podsiadlowski P., 1995, *MNRAS*, 273, 1041
 Reid I. N., Gizis J. E., Hawley S. L., 2002, *AJ*, 124, 2721
 Reid I. N., Lewitus E., Allen P. R., Cruz K. L., Burgasser A. J., 2006, *AJ*, 132, 891
 Reipurth B., 2000, *AJ*, 120, 3177
 Reipurth B., Clarke C., 2001, *AJ*, 122, 432
 Salpeter E. E., 1955, *ApJ*, 121, 161
 Scholz A., Jayawardhana R., Wood K., 2006, *ApJ*, 645, 1498
 Sterzik M. F., Durisen R. H., 2003, *A&A*, 400, 1031
 Thies I., Kroupa P., Theis C., 2005, *MNRAS*, 364, 961
 Umbreit S., Burkert A., Henning T., Mikkola S., Spurzem R., 2005, *ApJ*, 623, 940
 Weidner C., Kroupa P., 2004, *MNRAS*, 348, 187
 Weidner C., Kroupa P., 2006, *MNRAS*, 365, 1333
 Whitworth A., Bate M. R., Nordlund Å., Reipurth B., Zinnecker H., 2007, in Reipurth B., Jewitt D., Keil K., eds, *Protostars and Planets V The Formation of Brown Dwarfs: Theory*. pp 459–476
 Whitworth A. P., Stamatellos D., 2006, *A&A*, 458, 817
 Whitworth A. P., Zinnecker H., 2004, *A&A*, 427, 299